European Journal of Pharmaceutical Sciences 214 (2025) 107298

Contents lists available at ScienceDirect

European Journal of Pharmaceutical Sciences

journal homepage: www.elsevier.com/locate/ejps

Effect of hyaluronic acid on the performance of pulmonary surfactant. Towards the production of enhanced clinical surfactant formulations

Ainhoa Collada [a,b], Amaya Blanco-Rivero [a], Antonio Cruz [a,b], Jesús Pérez-Gil [a,b,*]

[a] Biochemistry and Molecular Biology Department, Faculty of Biological Sciences, Complutense University, Madrid, Spain
[b] Research Institute Hospital Universitario "12 de Octubre (imas12)", Complutense University, Madrid, Spain

ARTICLE INFO

Keywords:
Pulmonary surfactant
Polymers
Amniotic fluid surfactant

ABSTRACT

In order to prevent alveolar collapse, the surface tension at the air-liquid interface of alveoli has to be minimized at the end of expiration. Pulmonary surfactant, a lipid-protein complex synthetized and secreted by type II pneumocytes, adsorbs into the alveolar surface to form highly surface-active interfacial films. Lack or inactivation of surfactant is associated with severe respiratory pathologies, some of them treated by supplementation with exogenous surfactant formulations. It has been demonstrated that surfactant is assembled by pneumocytes in a highly packed dehydrated state that unravels once secreted to exhibit optimal interfacial capacities. Once exposed to air and subjected to dynamic breathing, surfactant can be isolated from bronchoalveolar lavages (BAL) in more unpacked and relatively hydrated stages. In this work we have used different biophysical techniques, such as surface balances and fluorescence spectroscopy to show how BAL surfactant pre-exposed to certain polymers such as hyaluronic acid (HA) transits to a more stably packed state with improved functional capabilities that approach those of freshly secreted surfactant that had never been exposed to air, such as the surfactant that can be purified from amniotic fluid. These results open new opportunities to develop more efficient therapeutical surfactant preparations to treat respiratory pathologies still unresolved.

1. Introduction

Pulmonary surfactant (PS) is synthetized by alveolar type II pneumocytes where it is stored in the form of lamellar bodies (LBs) that are specialized organelles in the form of tightly packed and dehydrated concentric membranes which contain surfactant lipids and proteins (Weaver et al., 2002). Once secreted, these complexes unravel to form interfacial films at the respiratory surface with the ability to reduce the surface tension to minimal values, especially at high compression stages, such as those reached at the end of expiration (Cerrada et al., 2015; Hobi et al., 2014; Ravasio et al., 2010).

As the lungs mature in the last weeks of the gestational development, very preterm newborn babies with immature lungs and lack of PS may develop the Neonatal Respiratory Distress Syndrome (NRDS) that caused the death of thousands of infants every year due to lung immaturity (Whitsett et al., 1986). The development of surfactant replacement therapies (SRTs) in which an exogenous surfactant is introduced intratracheally to facilitate the opening of the PS-lacking lungs while it stimulates the production of endogenous PS, turned the tables and the mortality was drastically reduced (Echaide et al., 2017).

SRTs have been used for the treatment of respiratory pathologies caused by the lack of an operative surfactant since more than forty years ago (Adams et al., 1978; Enhörning and Robertson, 1972; Fujiwara et al., 1980). However, these therapies still lack efficiency and optimization and result inefficient to treat some of the most important pathologies associated with surfactant disorder. For example, in Acute Respiratory Distress Syndrome (ARDS) as a consequence of lung injury and inflammation, or in babies born at term but suffering of meconium aspiration syndrome which ends in an strong inactivation of the endogenous PS, SRTs have not been proven effective since the exogenous surfactant introduced gets also inactivated (Baer et al., 2019; Willson and Notter, 2011).

Available clinical surfactants are subjected to high production cost, batch-to-batch variability and risk of pathogen transmission when obtained from natural sources (Seurynck-Servoss et al., 2007) as well as high susceptibility to inactivation, and therefore the production and optimization of improved formulations has been largely pursued. Possibilities proposed to improve existing surfactants include

* Corresponding author at: Department of Biochemistry and Molecular Biology, Faculty of Biological Sciences, Complutense University, José Antonio Novais 12, 28040 Madrid, Spain.
E-mail address: jperezgil@bio.ucm.es (J. Pérez-Gil).

https://doi.org/10.1016/j.ejps.2025.107298
Received 31 August 2025; Received in revised form 23 September 2025; Accepted 26 September 2025
Available online 27 September 2025
0928-0987/© 2025 The Authors. Published by Elsevier B.V. This is an open access article under the CC BY-NC-ND license (http://creativecommons.org/licenses/by-nc-nd/4.0/).

supplementation with lipid components (Rüdiger et al., 2005) or the incorporation of certain additives. Different studies showed for instance that the exposure to certain polymers can potentiate surfactant activity, including the promotion of a higher resistance to inactivation (Kobayashi et al., 1999; Lu et al., 2005a; William Taeusch et al., 1999; Zuo et al., 2006). In this work we have decided to investigate the effect of hyaluronic acid (HA) in PS structure and function to get further insight into the possibility of using it as additive for improved SRTs. HA is an ionic polymer naturally found in the lung, what confers it with the ability to interact with surfactant complexes in pathological and non-pathological contexts (Bjermer et al., 1989; Hällgren et al., 1989; Turino and Cantor, 2003). It has been shown that exposure of PS to relatively low concentrations of HA is enough to produce beneficial effects in terms of surface activity and resistance to inactivation (Braun et al., 2007; Taeusch et al., 2008), and that this apparent activation is associated with HA-promoted higher packing and dehydration states (Lopez-Rodriguez et al., 2013).

It was shown that PS isolated from animal bronchoalveolar lavages (BAL) does not retain the highly packed structure of recently secreted LBs (Cerrada et al., 2015), which is at least partly maintained by surfactant that has been secreted but still not exposed to air-liquid interfaces, such as the surfactant that can be purified from amniotic fluid (Castillo-Sánchez et al., 2022). In this work we wanted to study how the exposure to HA of a native surfactant isolated from BAL of porcine lungs affects its adsorption and spreading capabilities and compare these effects with the behavior of a human amniotic fluid surfactant that preserves the structural determinants of a newly synthetized material with optimal functional capabilities. The results obtained could pave the way for the production of a new generation of clinical surfactants with higher activity and enhanced potential to treat pathologies that challenge PS function.

2. Materials and methods

2.1. Materials

Hyaluronic acid (HA) from *Streptococcus zooepidermicus* (H9390, Sigma) was diluted in buffer Tris 5 mM, NaCl 150 mM, pH 7.4 and preserved at −20 °C. When required, it was added at 0.25 % (w/v). The concentration chosen for HA (w/v) was that found effective to promote resistance of surfactant to inactivation in previous studies (Lu et al., 2005a, 2005b; Lu and Taeusch, 2010). Stocks of the fluorescent probe FM1–43 (Molecular Probes Inc., catalog number T3163) were prepared in DMSO and stored in glass vials at −20 °C. Native surfactant (NS) was isolated from bronchoalveolar lavages (BAL) obtained from porcine lungs by a protocol optimized at our laboratory (Taeusch et al., 2005). In brief, each pair of lungs was washed with 2 L of a buffer solution (Tris 5 mM, NaCl 150 mM, pH 7.4) by vigorously massaging them and the resulting lavage was filtered. To obtain pulmonary surfactant from these lavages, first, cells and debris were removed by centrifugation (5 min, 1000 g, 4 °C). Then, BAL were ultra-centrifuged in an angular rotor (100,000 g, 4 °C, 1 hour) to pellet high-density surfactant complexes and membranes. Afterwards, pellets were homogenized using a potter and charged into a NaBr discontinuous density gradient containing the solutions: NaBr 16 % (w/v) in NaCl 0.9 %; NaBr 13 % in NaCl 0.9 % and NaCl 0.9 %. Tubes were ultra-centrifuged for 2 h in a swinging rotor at 120,000 g and 4 °C. Purified NS complexes were located between the second and third gradient solutions. They were recovered, aliquoted, frozen in liquid N_2 and stored at −80 °C until employed. Amniotic fluid surfactant (AFS) was obtained in a non-invasive way from programmed C-sections at term in collaboration with the Obstetrics and Gynaecology Service of Hospital 12 de Octubre (Madrid, Spain) upon informed consent of the donor mothers. The collected amniotic fluid, whose total volume varied upon samples, was carried to the laboratory and AFS was isolated following the same protocol than for NS. Both NS and AFS quantification was performed by phosphorus analysis (Rouser et al., 1966).

3. Methods

3.1. Sample preparation

NS and AFS samples were unfrozen and diluted to optimal concentration in buffer. For HA addition, an aliquot of NS was put into contact with 0.25 % HA (w/v) by vortex agitation during 1 min to facilitate HA incorporation into NS membranes (NS + 0.25 % HA). For its elimination (NS - 0.25 % HA), a 30 min centrifuge at 14,500 g and 4 °C was performed. The supernatant containing buffer + HA was discarded and the NS membranes that pelleted, resuspended in the same amount of buffer solution that was removed. The buffer solution used in all experiments was Tris 5 mM, NaCl 150 mM, pH 7.4.

3.2. Fluorescence spectroscopy

NS, with or without HA, and AFS were diluted to the desired final phospholipid concentrations (in the range between 0 and 50 μg/ml) with buffer. The fluorescent probe FM1–43 was then incorporated to the samples at a concentration of 2.4 μM and the tubes were vortexed and incubated at 37 °C for 30 min in dark conditions before the fluorescence emission was measured. Fluorescence measurements were done in an Aminco Bowman luminescence spectrometer thermostated at 37 °C. Emission spectra were recorded using 4 nm excitation and 8 nm emission slitwidths and adjusting the same sensitivity for all measurements. Phospholipid concentration was checked by phosphorus quantification (Rouser et al., 1966) and the maximum fluorescence ($\lambda ex = 479$ nm, $\lambda em = 600$ nm) was plotted versus lipid concentration.

3.3. Surfactant adsorption and accumulation test

The capability of different preparations to adsorb and accumulate at air-liquid interfaces was assessed thanks to a modified surfactant adsorption test (Autilio et al., 2017; Ravasio et al., 2008). In this protocol, each well of a multi-well plate is filled with 80 μl of Brilliant Black (Sigma Aldrich, St. Louis, Missouri, USA), a quencher of fluorescence. Samples are stained with the fluorescent dye BODIPY-PC (Molecular Probes, Life Technologies, CA, USA, catalog number A10072) at 2 % mol with respect to phospholipid as it was found to be an optimal concentration for a proper sensitivity (Autilio et al., 2017). The staining was performed by incubation during 1 hour in a Thermomixer (Eppendorf; Hamburg, DE) at 37 °C and intermittent agitation (1400 rpm every 10 min). After that, the sample is diluted in working buffer and a total of 3 μg of lipid in 20 μl are injected in each well with an automatic pipette with special care in depositing the material at the bottom of the well. After injecting every sample, the plate is introduced in a FLUOstar OPTIMA Microplate Reader (BMG Labtech, Offenburg, Germany) thermostatized at 37 °C and a measurement of the fluorescence intensity at the interface as detected from above is performed every 2 min during 1 hour. As Brilliant Black has no surface activity, an increase in fluorescence should be observed if the material adsorbs into the interface and BODIPY-PC molecules escape from the quencher at the bulk phase (Ravasio et al., 2008). Experiments were performed by triplicate and data are plotted as relative fluorescence units (RFU) versus time after subtraction of the background contribution.

3.4. Adsorption surface balance

A Wilhelmy balance made of Teflon with an area of 3.14 cm^2 was employed to study the interfacial adsorption of different preparations in the presence or absence of HA. The trough was filled with 1.9 ml of buffer solution. Then, 10 μg of the samples were injected onto the subphase of the balance and the changes in surface pressure were monitored against time thanks to the use of a Wilhelmy plate of 24 mm x 10 mm x

0.5 mm made of grade 41 Ashless Filter Paper (Whatman, GE, Healthcare Life Sciences) previously attached to the pressure sensor. Experiments were performed at 37 °C with a magnet moving to agitate the subphase and facilitate the incorporation of material onto the interface without diffusion limit.

3.5. Spreading surface balance

The spreading capabilities of the different materials with or without previous exposure to HA were evaluated thanks to the use of a spreading trough with a special design consisting of a donor trough connected by a continuous zigzagging path to a receptor trough (mimicking the upper and distal airways respectively) (Fig. 1). Both, donor and receptor troughs are probed by a paper pressure sensor that detects changes in surface pressure (García-Mouton et al., 2023). The trough is filled with 54 ml of buffer and thermostated to 25 °C. Then, the material is injected into the donor trough using a Hamilton microsyringe and the changes in surface pressure in both, donor and receptor trough, are monitored against time.

3.6. Compression-expansion isotherms

The behavior of PS films subjected to compression and expansion was studied using a Langmuir-Blodgett trough of 213 cm^2 (Nima Technology, Inc., Coventry, England) (López-Rodríguez et al., 2016) containing 400 mL of buffer solution and delimited by a mobile continuous Teflon ribbon barrier, able to compress the films to maximal pressures with no leakage. All the experiments were conducted at constant temperature of 25 °C thanks to an external circulating water bath. A Wilhelmy plate made of grade 41 Ashless Filter Paper (Whatman, GE, Healthcare Life Sciences) was used as pressure sensor. Interfacial monolayers were formed by spreading drops of the sample on the interface using a Hamilton microsyringe until reaching 50 μg of lipid and left to equilibrate for 10 min. After that, films were subsequently compressed and expanded at a rate of 65 cm^2/min while surface pressure was recorded. This rate is still far from physiological but allows observing rearrangements occurring at the interfacial level due to compression-expansion dynamics.

3.7. Captive bubble surfactometry

In this device, an air bubble whose surface defines an air-liquid interface is created inside an assay chamber thermostated at 37 °C containing a degassed buffered solution with 10 % sucrose (w/v) to increase density. A small amount of sample (150 nL at 20 mg/ml) is then injected with a microcapillar below the bubble surface and its initial adsorption onto the interface is monitored for 5 min following the changes in shape of the bubble recorded by a digital videocamera. Then, the chamber is sealed and the bubble is subjected to a quick expansion (~25 % of its volume). Post-expansion adsorption is again monitored for 5 min. Finally, compression-expansion cycles are carried out. First, 4 quasistatic cycles where the bubble is reduced or enlarged at a slow speed and then dynamic cycles are performed at 20 cycles/min mimicking physiological breathing conditions. Finally, a stability test was performed by mechanically perturbing the bubble with a pendulum hammer and measuring the variations in its shape and size upon the different perturbations applied (Schürch et al., 2010).

Surface tension, volume and area are calculated by measuring the height and the diameter of the bubble thanks to a specific software (Schoel et al., 1994). Initial adsorption and post-expansion adsorption graphs are represented as surface tension vs. time after averaging data from three independent replicas. In the case of cycling experiments, graphs show surface tension vs. area and graphs correspond to representative experiments from three replicas. In dynamic cycling, only the 1st, 10th and 20th cycles are represented in the figures for clarity (Hidalgo et al., 2017).

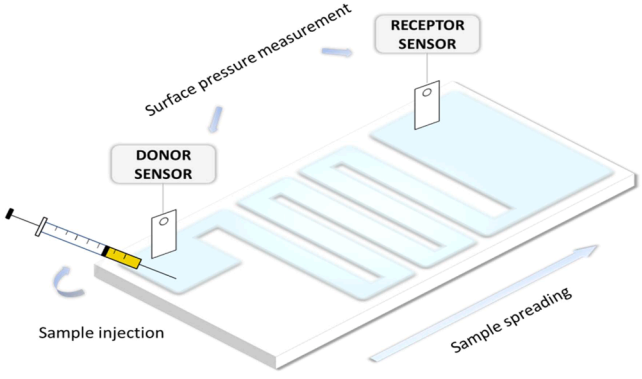

Fig. 1. Schematic representation of the spreading trough. The donor and receptor compartments are interconnected by a zigzagging path and the changes in surface pressure in the receptor trough upon injection of the material in the donor compartment are monitored against time.

3.8. Differential scanning calorimetry

Experiments were performed in a microcalorimeter (MicroCal VP-DSC, Amherst, MA, USA) with buffer in the reference cell and PS at 1 mg/ml with or without HA in the sample cell. Several scans were performed by sample starting from a temperature of 15 °C and reaching a final temperature of 70 °C, with a scan rate of 30 °C/hour, and pre- and post-scan thermostatizing time during 5 min. A representative scan was plotted for each sample using Origin 7 (Origin Labs, Northampton, MA, USA).

4. Results

4.1. Fluorescence spectroscopy

The reorganization of surfactant membranes caused by the exposure to HA was investigated thanks to the use of the fluorescent probe FM1–43. This probe is water-soluble but increases fluorescence emission several folds once it binds to lipid bilayers, being its fluorescence quenched by water molecules when it is free in the solvent (Henkel et al., 1996). However, due to its high polarity it is unable to translocate and bind to inner membranes, so it only labels the external leaflet of membranes in vesicles. In this way, an increase in fluorescence can be associated to an increase in the membrane surface accessible to the dye, thus, increased permeability. Fig. 2 shows the fluorescence emission of FM1–43 as a function of the phospholipid concentration for NS membranes not exposed to HA, in the presence of HA (+ 0.25 % HA), after exposure and removal of HA (- 0.25 % HA) and for AFS membranes.

NS membranes that have not been exposed to HA promote maximal fluorescence of FM1–43 indicating exposure of a larger outer surface available for binding to the probe. The presence of HA reduces significantly the phospholipid-dependent increase in fluorescence, indicating that the polymer has induced reorganization of the membranes, likely including vesicle aggregation, which reduces the proportion of the surface that is accessible to the probe. Interestingly, the removal of HA from the pre-exposed samples does not revert the polymer effect, suggesting that polymer-promoted reorganizations are permanent. This permanent effect of HA on NS membranes makes them to approach the accessibility to FM1–43 exhibited by AFS complexes, a material that was found to have maximal packing and dehydration (Castillo-Sánchez et al., 2022).

4.2. Interfacial adsorption

The adsorption capabilities of NS membranes into air-liquid

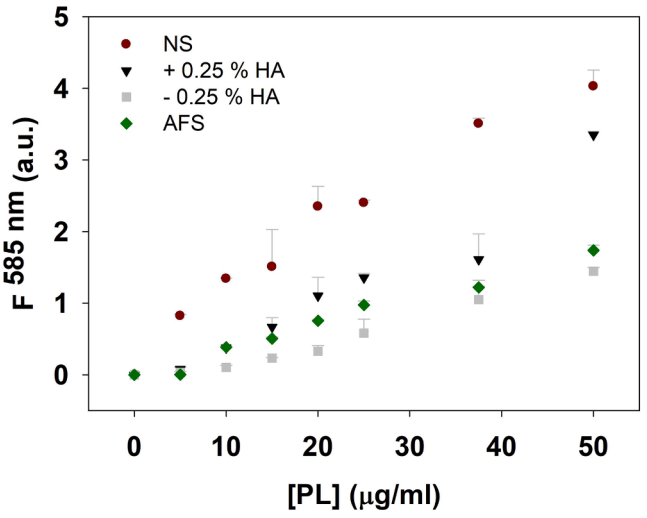

Fig. 2. Fluorescence emission of FM1–43 upon binding to different amounts of NS ± 0.25 % HA or AFS membranes.

interfaces were evaluated in the presence or absence of HA thanks to the use of two different techniques that measure the adsorption to the interface of the material previously deposited into the subphase. The Surfactant Adsorption and Accumulation Test (SAAT) measures the increase in fluorescence associated with the arrival of fluorescently-labeled material to the interface as it escapes from a quenching agent diluted in the bulk liquid phase. In the Wilhelmy trough, adsorption into the interface is monitored by the concomitant increase in surface pressure (reduction in surface tension). The results of these adsorption experiments are summarized in Fig. 3.

In the SAAT experiments (Fig. 3, **left**) AFS shows the maximum initial rate of accumulation of material at the interface, which slowly decays with time to equilibrium values that are also reached by NS at longer times. After 50 min, the interface gets fully covered of material in all cases and no increase of fluorescence is detected anymore. The presence of HA seems to impair the arrival and accumulation of NS to the interface, possibly as a consequence of the changes in viscosity and concomitant limits to diffusion imposed by the polymer, which does not allow the large surfactant complexes to fully escape from the quenching environment of the bulk. Interestingly, the removal of HA permits again NS to reach the interface, even at faster initial rates that those initially shown by NS that had never been exposed to the polymer. The direct measurement of changes in surface tension and surface pressure as a consequence of adsorption reflects similar effects of HA as seen in the Wilhelmy trough (Fig. 3, **right**). Again, AFS showed also in these experiments the maximal capabilities to adsorb into the interface and increase surface pressure (see Table 1). NS adsorbs at much slower rate, reaching only 2.2 ± 0.7 mN/m in the first 2 min of experiment, which is significantly accelerated by the exposure to HA (4.1 ± 1.6 mN/m), and especially enhanced after its elimination (10.5 ± 3.3 mN/m) to approach, at least in the first minutes, the adsorption rates reached by AFS. This HA-promoted enhanced NS adsorption is partly maintained after HA withdrawal.

4.3. Interfacial spreading

The capability of the different surfactant samples to spread once adsorbed to the interface was assessed thanks to a newly designed trough with a zigzagging path that connects donor and recipient compartments through a continuous interface (Fig. 1). The design somehow mimics how surfactant secreted at the alveolar spaces can travel to long distances and coat the whole respiratory surface upon adsorption into the interface and spreading associated to it. In the case of clinical surfactants used for SRT, interfacial spreading is important for the surfactant delivered endotracheally at the upper airways to distribute along the whole respiratory surface and reach the distal airways at the deep lung. This assay to test interfacial spreading capabilities has been used to probe the efficiency of surfactant to promote the delivery of inhaled drugs using the air-liquid interface as a pathway (García-Mouton et al., 2023; Hidalgo et al., 2021).

The time (s) of stabilization of surface pressure in the receptor compartment was calculated as the first time point at which surface pressure at the receptor compartment differs in less than 1 mN/m from the value of surface pressure in the donor compartment, and the surface pressure of stabilization (mN/m) was taken as the first time point in which surface pressure between donor and receptor compartments varies in less than 0.3 mN/m. Obtained from the analysis of data in Fig. 4.

As it can be seen in Fig. 4, the amount of NS deposited at the donor trough adsorbs rapidly at the interface to pressures close to 10 mN/m that then decays as the surface pressure starts to increase at the recipient compartment. This is indicative of spreading along the interfacial pathway until surface pressure in the two compartments fully

Table 1
Surface pressure (in mN/m) upon adsorption ($t = 2$ min) and at the end of the experiment ($t = 16$ min) derived from all samples tested in the Wilhelmy trough.

	$t = 2$ min	$t = 16$ min
NS	2.2 ± 0.7	9.5 ± 1.2
NS + HA	4.1 ± 1.6	12.5 ± 3.7
NS – HA	10.5 ± 3.3	15.4 ± 0.6
AFS	14.0 ± 1.8	20.7 ± 0.7

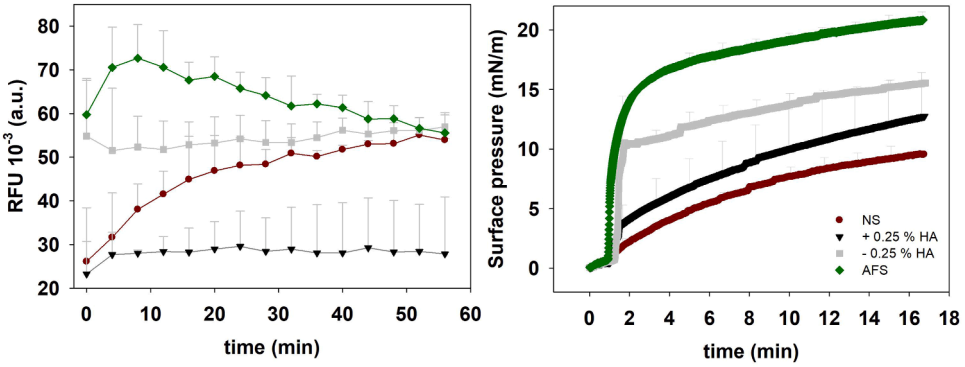

Fig. 3. Interfacial adsorption of NS in the absence or presence of HA and of AFS in the surfactant adsorption test (left) or in the Wilhelmy trough (right). The adsorption kinetics are monitored against time and plotted as relative fluorescence units in the case of SAAT or surface pressure in the case of the Wilhelmy trough experiments, being in both cases an increase in fluorescence or surface pressure an indicator of a higher amount of material arriving at the interface.

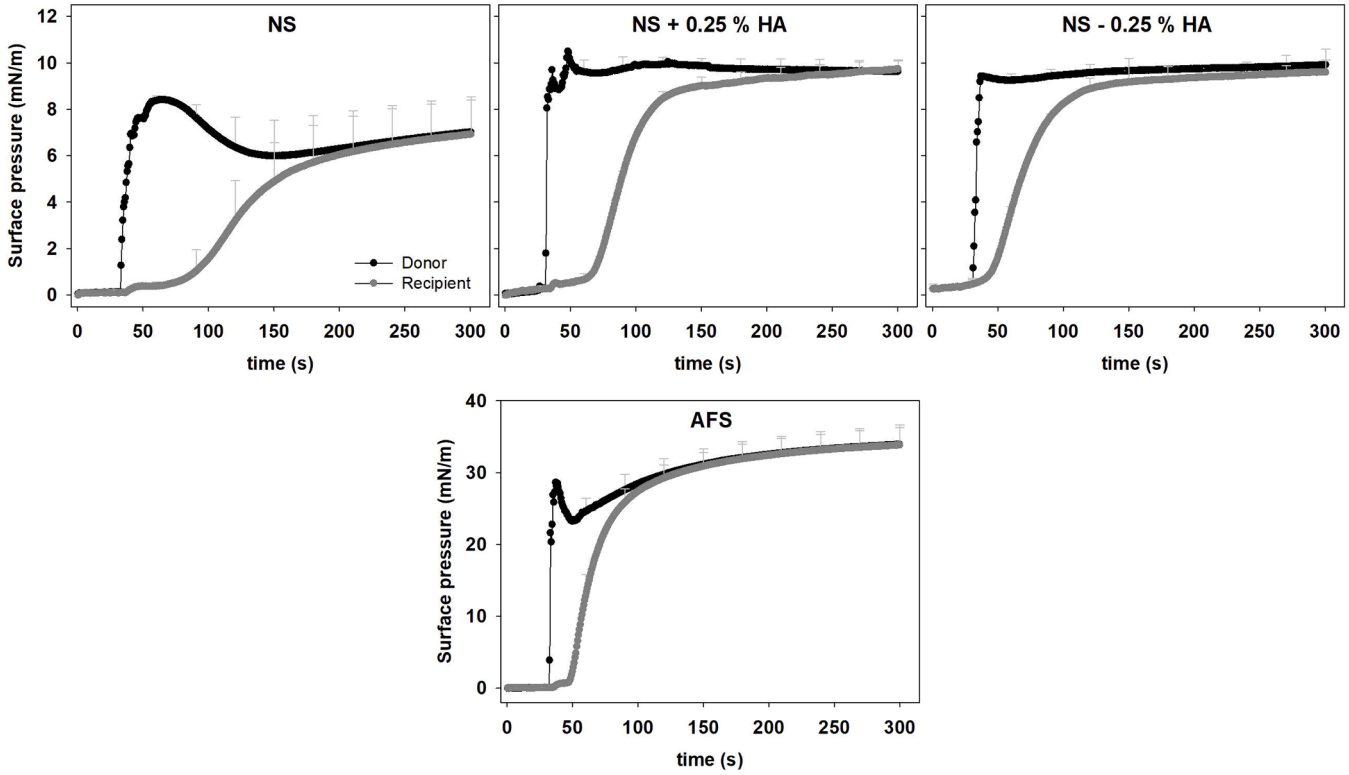

Fig. 4. Comparison of the interfacial spreading capabilities of NS, in the absence or presence of HA, and of AFS.

equilibrates. The lag time between the increase in pressure in donor and recipient compartments reflects the efficiency and rate of spreading through the connecting pathway. The sample of NS exposed to HA adsorbs to higher pressure as it is deposited in the donor compartment (9.7 ± 0.5 mN/m), and produces an earlier increase of pressure at the recipient compartment, with a shorter lag time than it produced in the absence of HA (138 s). That means that the reorganization induced by HA in NS complexes yields a more efficient material not only in terms of adsorption as we had seen above, but also in terms of interfacial spreading. Remarkably, this activation induced by HA is retained upon removal of the polymer, as the stabilization surface pressure maintains between samples of NS + HA and NS – HA (see Table 2). The HA-promoted enhancement of interfacial spreading goes in the direction of the activity of AFS, although AFS still exhibited the most efficient spreading activity, producing an immediate increase in surface pressure to values above 30 mN/m in the donor and recipient compartments with a minimal lag period (Table 2).

4.4. Compression-expansion isotherms

Cyclic compression-expansion isotherms of the interfacial films formed by the different samples in a surface balance were obtained in order to study the effect induced by HA on the capability of surfactant complexes to form operative films able to reach and sustain low surface tensions (high surface pressures). 50 μg of material were spread at the interface as it was seen to be enough to reach surface pressures above the typical 2D-to-3D transition plateau exhibited by surfactant at around 45 mN/m (Castillo-Sánchez et al., 2025). As it can be observed in Fig. 5, the compression isotherm of NS that had not been exposed to polymers shows a conspicuous plateau at 45 mN/m that informs about the reorganization of the material at the interface. In that way the air-exposed monolayer results depurated of the less surface-active species, becoming competent to produce the highest surface pressures. Subsequent cycles reach a bit lower surface pressures (see inset in Fig. 5**, top left**), meaning that some material has been lost towards the subphase. The exposure of NS to HA produced a reduction in the exclusion plateau occurring at 45 mN/m of around a 20 % of its total length in comparison with NS and also an overlap in subsequent cycles (see inset in Fig. 5**, bottom left**). That means that the films formed by the material reorganized as promoted by HA require less reorganization at the plateau to become capable of sustaining the highest pressures. Also, that upon compression-expansion cycling, less material is lost to the bulk between subsequent cycles. Thus, the polymer seems to reduce the hysteresis of the cycles but only when it is in contact with NS, because after its removal, NS seems to revert to the previous behavior. In contrast, the cyclic isotherms produced by AFS films turned out to be less hysteretic, indicating a more limited reorganization of the complexes at the interface and less material lost between cycles, finding also a much more discrete plateau. This behavior is associated with a better performing surfactant.

Table 2
Parameters defining the spreading of surfactant materials in the absence or presence of HA.

	t (s)	Surface pressure (mN/m)
NS	152	6.2 ± 1.6
NS + HA	138	9.7 ± 0.5
NS – HA	106	9.8 ± 0.5
AFS	98	31.1 ± 2.2

4.5. Captive bubble surfactometry

Initial (IA) and post-expansion (PEA) adsorption of NS in the absence or presence of HA showed the immediate reduction of the surface tension to the equilibrium surface tension values (Fig. 6). Exposure to HA reduced the minimal surface tension reached after 5 min of adsorption from 25–27 mN/m to around 23 mN/m, both upon initial adsorption to a clean bubble and upon expansion of the bubble. Interestingly, the ability to reach lower surface tension was maintained upon removal of

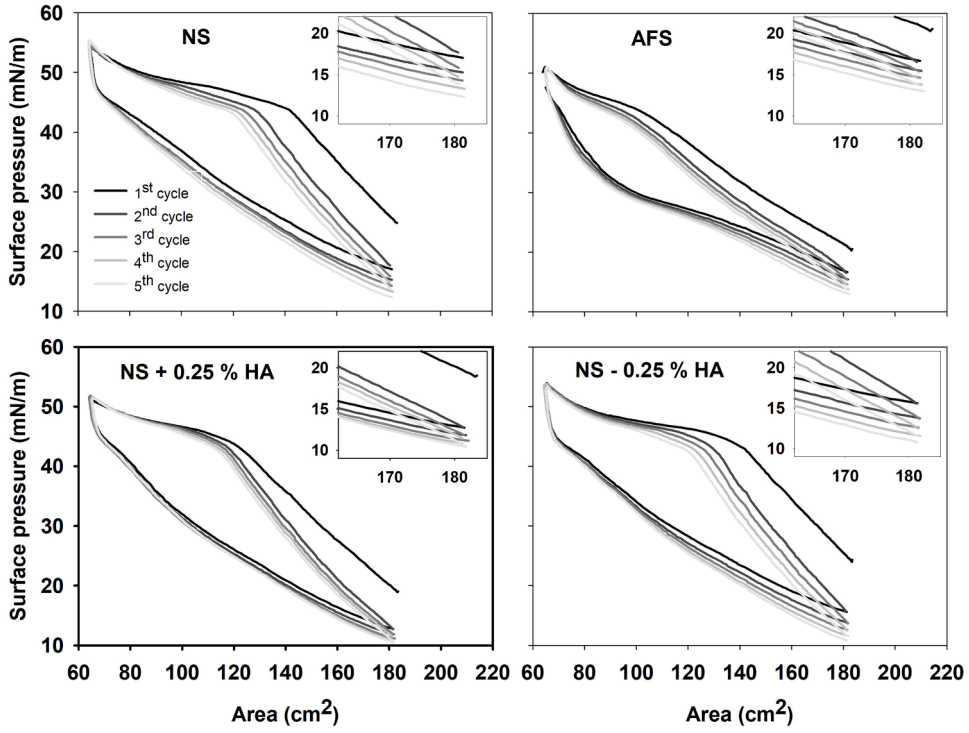

Fig. 5. Cyclic compression-expansion isotherms of films formed by NS, in the absence or presence of HA, and by AFS. Insets replot values at large surface area for better visualization of differences at the end of expansion.

the polymer from the NS samples.

Quasistatic cycles show how NS films reduce the surface tension to very low values since the first cycle. This first cycle exhibits some hysteresis, likely associated with a reorganization of the material at the interface, which is maintained in subsequent cycles, where compression is directly converted into very low tension with almost no hysteresis. In the presence of HA, NS films are also competent to produce very low surface pressures, although the area reduction required is higher resulting in a larger hysteresis of the first cycle. This means that probably part of the compression work is applied to squeeze the polymer away from the film and/or reorganize in a different manner the structure of the surface-associated structures as they were modified by HA exposure. However, and somehow surprisingly, once the polymer was removed from NS samples, the corresponding films showed even more marked hysteresis when compressed to the slow rates of the quasi-static regime. Nevertheless, when the samples were subjected to dynamic cycles, at compression rates comparable to those supposedly occurring during breathing, all showed optimal behavior defined as reaching less than 3 mN/m of minimal surface tension with less than 20 % area reduction.

Fig. 7 presents the data of the stability tests carried out with bubbles compressed to minimal surface tension during dynamic cycles and then subjected to consecutive discharges of a pendulum hammer that produces shocking mechanical perturbations. NS forms stable surface films that can maintain, upon compression, very low surface tensions, maintained below 5 mN/m even after a few shocking hits. Exposure to 0.25 % (w/v) of HA seems to slightly affect the stability of the NS films, but it is enhanced upon removal of the polymer.

4.6. Thermotropic transitions

Differential Scanning Calorimetry (DSC) was used to analyze the thermotropic transitions between lipid phases in NS membranes before, during and after exposure to HA. These transitions and their parameters are very sensitive to the organization of surfactant membranes, which should offer clues of the nature of transformations induced by the polymer into surfactant complexes. The DSC thermograms obtained are compared in Fig. 8 and the parameters calculated from the main ordered-to-disordered transition are summarized in Table 3.

NS membranes have a well characterized thermotropic behavior, with a broad and asymmetric ordered-to-disordered transition that ends very close to physiological temperature. HA turned out to have a significant effect on NS thermotropic behavior. First, HA increases the enthalpy of the transition in a significant manner once it is interacting with NS, from around 3 to above 4 Kcal/mol, with a slight shift of the T_m to higher temperature, from 30 to 31 °C. This means that exposure to HA likely produces an increase in packing of the membranes, that stabilizes the ordered phase. Upon removal of the polymer, the enthalpy returns to the original NS values but the T_m keeps being significantly higher than that of NS that had not been exposed to HA. That means that some of the structural transformations induced by the exposure to polymers are irreversible, but not others.

5. Discussion

Since the 80′s, the possibility to supplement native surfactants with additives to enhance its activity, as different phospholipids or even surfactant proteins, was taken into consideration (Chung et al., 1989; Morley et al., 1980) setting the basis of a line of research that is still open nowadays. The use of polymers as additives was introduced in the late 90′s (Kobayashi et al., 1999; William Taeusch et al., 1999). Since then, extensive research has focused in describing their mechanism of action and their optimal doses. As HA had been shown to revert the inhibition caused by serum or meconium on PS performance in an irreversible way with only pre-incubation (Lopez-Rodriguez et al., 2013), we found it interesting to directly compare the effect of HA both, upon direct contact and after exposure, on our NS preparation obtained from animal BAL and to compare its behavior with that of a human surfactant with enhanced capabilities.

Although different polymers have been studied as possible additives to PS membranes, in this study HA was chosen because it is a polymer naturally present in the context of the lung, secreted by alveolar

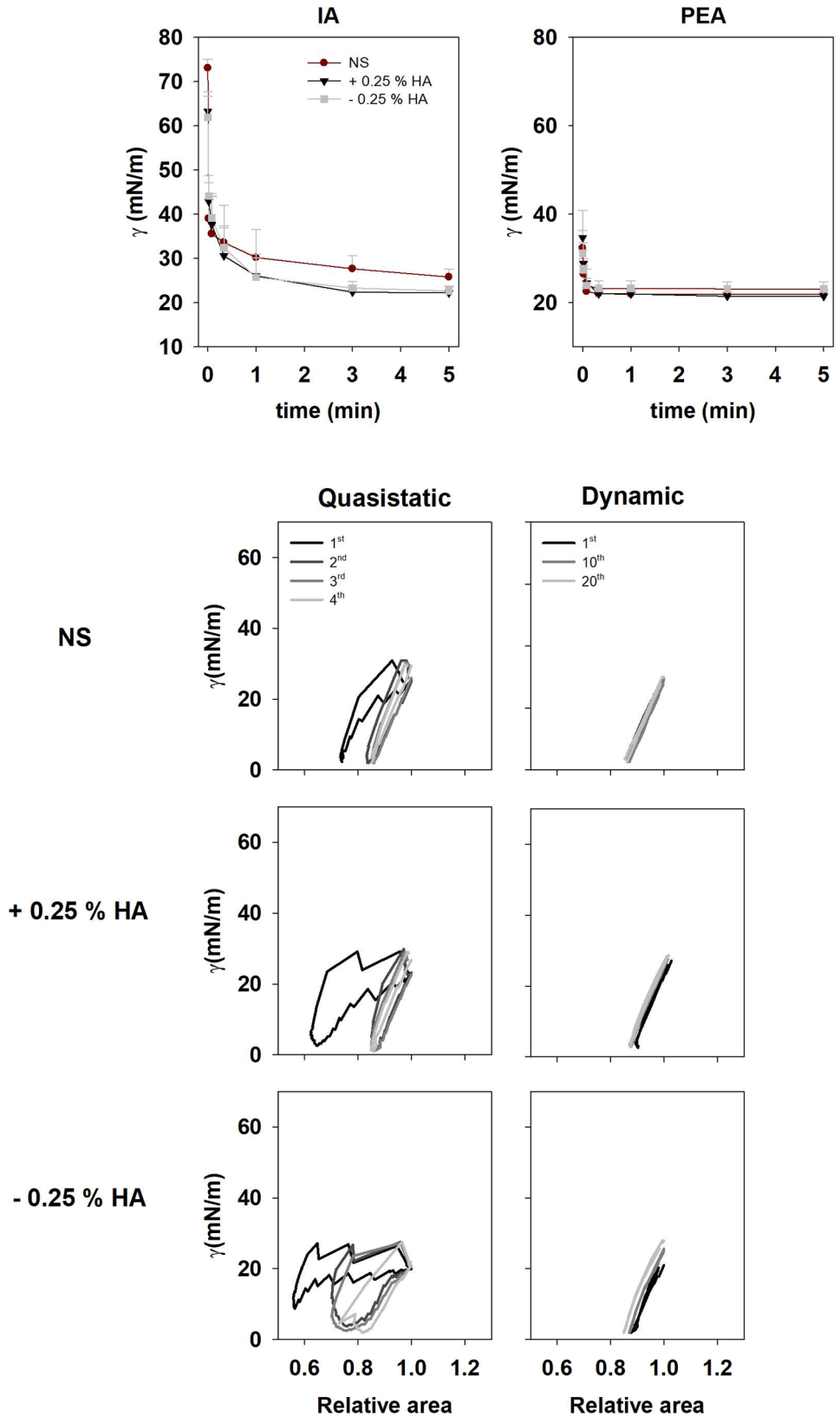

Fig. 6. Top: initial adsorption (IA) and post-expansion adsorption (PEA) of NS with or without exposure to 0.25 % HA. Bottom: Quasistatic and dynamic cycles of films formed by NS in the absence and presence of HA. Only a representative replicate is shown for clarity ($n = 3$).

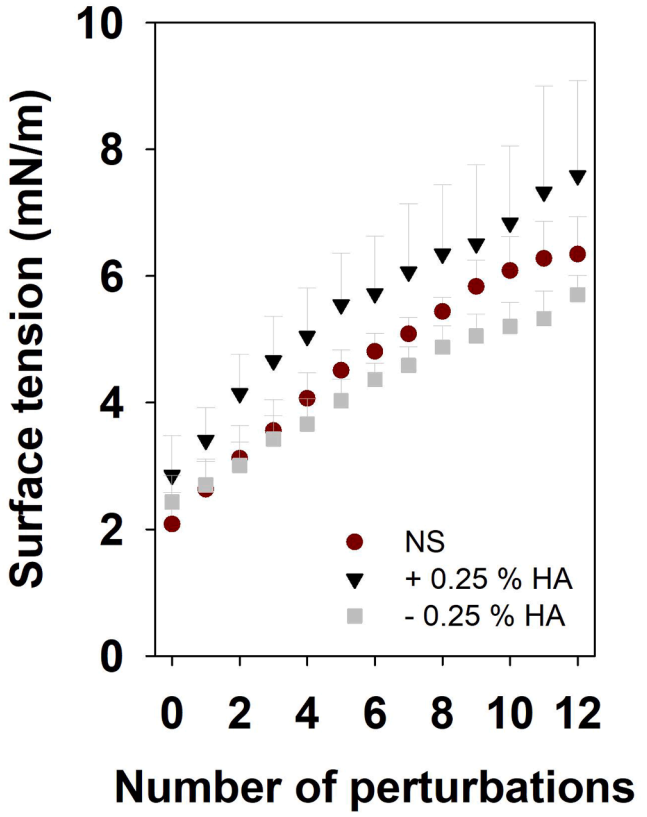

Fig. 7. Mechanical stability of films made of NS, in the absence or presence of HA. Plotted is the minimal surface tension produced upon compression of bubbles coated with the different tested materials before (0) and after the introduction of an increasing number of mechanical perturbations by discharge of a pendulum hammer onto the chamber of the CBS.

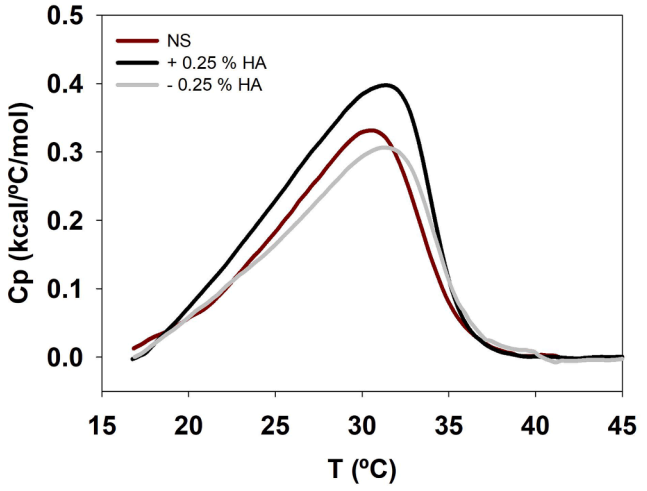

Fig. 8. DSC thermograms of NS, NS + 0.25 % HA and NS – 0.25 % HA. A representative thermogram is represented for each sample.

Table 3
Parameters obtained in the DSC experiments. Results are expressed as mean and SD for $n = 10$. ** refers to $p < 0.001$ and * to $p < 0005$ by the t-student test.

	ΔH (kcal/mol)	T_m (°C)	$\Delta T_{1/2}$ (°C)
NS	3.3 ± 0.3	30.1 ± 0.3	9.6 ± 0.5
+ 0.25 % HA	4.1 ± 0.2**	31.0 ± 0.4**	10.2 ± 0.2*
- 0.25 % HA	3.2 ± 0.2	31.3 ± 0.3**	9.9 ± 0.3

epithelial cells (Sahu et al., 1980) being relevant to sustain the structure of alveolar spaces. HA is not surface active, what allows discerning the surface-active effects induced in surfactant complexes. Furthermore, anionic polymers such as HA have shown better capabilities at enhancing PS adsorption and reversing inhibition in lower concentrations than PEG (Braun et al., 2007; Taeusch et al., 2008), which has been interpreted as a function of its longer persistence length (Lopez-Rodriguez et al., 2013).

As largely discussed in the literature, polymers can induce PS membranes to rearrange, causing their dehydration and creating an osmotic pressure gradient between the media and the water inside PS membranes (Braun et al., 2007). In the case of HA, it forms networks in aqueous solutions by interactions with itself (Lu et al., 2009; Scott et al., 1991), producing the membrane aggregation and reorganization effects such as those seen in Fig. 2 that led to better adsorption and spreading capabilities (Figs. 3, 4 **and** 5) of the complexes to which the polymer had been exposed. Apart from the dehydrating effects caused by polymer-induced osmotic stress, surfactant reorganization has been also associated with entropic effects caused by depletion forces by polymer concentrations above their entanglement threshold (López-Rodríguez et al., 2012; Stenger and Zasadzinski, 2007; Yadav et al., 2024). This means that the polymer, above a certain concentration, could attract hydration molecules thus disrupting the osmotic balance in the system, favoring in this way lipid adsorption, as lipid molecules would then feel more attracted to the interface. Entropic-driven and osmotic-driven structural changes would end in reorganization of membrane complexes and membrane phases that are not reverted once the polymers are removed.

A good surfactant needs to have optimal interfacial adsorption and spreading capabilities to withstand the demanding conditions of breathing. HA had already been demonstrated to enhance PS adsorption; however here we have demonstrated that this adsorption enhancement still remains after polymer withdrawal (Figs. 3 **and** 4), especially in the case of the surfactant adsorption test (Fig. 3, left) where the presence of HA seemed to act as a barrier to the adsorption of the sample, probably due to the relatively high viscosity of the sample. Although not specifically studied here, viscosity of surfactant preparations in the presence of HA should be taken into account as it could affect SRT administration (Lu et al., 2009). However, if a pre-incubation step is enough to get an improved surfactant, even if some polymer molecules could persist associated to the sample, the ultimate removal of the polymer could avoid the problems associated to a intrinsic high viscosity of polymer-containing preparations. The enhanced capabilities of NS after polymer removal seen in this work have to be compared with the potential effect of polymers on other surfactant formulations, such as those reconstituted by synthetic lipids and synthetic or recombinant proteins or peptides, with the highest potential to constitute the basis for the new generation of clinical surfactants.

Many of the transformations and enhancements promoted by HA into NS approach its functional behavior to that of AFS complexes, the surfactant reported to exhibit best performance and thought to correspond to material that has been secreted by alveolar cells but has not been yet used at respiratory air-liquid interfaces. As a matter of fact, the performance of AFS seems to be far better than the one of NS even in the presence of HA. AFS membranes outdid NS with or without HA in terms of adsorption (Fig. 3, Table 1), indicating that the possible aggregates formed by the exposure of NS to the polymer do still not fully mimic the ones in AFS membranes, and spreading (Fig. 4, Table 2), where not only the highest surface pressures at which the different systems equilibrated upon spreading of equivalent amounts of material, but also the velocity at which this equilibration occurred was faster for AFS (Table 2). Further to this, surfactant re-spreading experiments (Fig. 5) also highlighted the enhanced capabilities of AFS to rapidly adsorb and desorb from the interface without great efforts and how the presence of the polymer helped to achieve a similar behavior in NS membranes to that of AFS ones. AFS once again showed the more efficient compression-driven

structural rearrangements with the exclusion plateau virtually disappearing, what could be related to the higher packing state of this material. AFS complexes have never been exposed to the air-liquid interface, so their organization would still preserve that of a newly synthetized material in the form of highly packed and dehydrated membranes with optimal adsorption capabilities (Castillo-Sánchez et al., 2022; Cerrada et al., 2015). Exposure of NS to HA could recapitulate part but not all of the highly packed assemblies present in freshly secreted surfactant, and this could explain why the behavior promoted by HA in NS membranes is in some way an intermediate between that of NS and AFS. Still, the transformations introduced seem to enhance some important properties, as the stability of interfacial films subjected to breathing-like compression-expansion dynamics such as those mimicked by the CBS (Figs. 6 **and** 7).

AFS can be considered a super-active material that could in principle have all the advantages for its use as a human surfactant for SRT, and some trials were in this sense developed to treat babies with NRDS (Schneider et al., 1982). However, AFS is obtained in little amounts and presents high variability between batches. These problems as well as the potential risk of transmission of pathogens makes difficult to consider AFS as an appropriate material for SRT. The production of enhanced clinical surfactants with much more controlled composition but optimized in terms of structure and biophysical properties by including in their production the appropriate (transient) exposure to polymers opens new possibilities that should be further explored in order to produce a next generation of enhanced clinical surfactant preparations.

All in all, our study suggests that pre-incubation with HA would be a good alternative for SRT development while the limitations of the use of a human surfactant for SRTs are overcome.

6. Conclusion

In this work the effect of the ionic polymer HA on the performance and behavior of NS complexes was analyzed when being in contact or after pre-exposure and removal of the polymer from PS membranes. The results obtained confirm that this polymer enhances PS adsorption and spreading capabilities even after its elimination, approaching the behavior of AFS, whose performance was still superior in all cases. These results could be useful in order to develop new improved therapeutic surfactant formulations.

CRediT authorship contribution statement

Ainhoa Collada: Writing – review & editing, Writing – original draft, Methodology, Investigation, Formal analysis, Conceptualization. **Amaya Blanco-Rivero:** Investigation, Formal analysis. **Antonio Cruz:** Writing – review & editing, Supervision, Formal analysis, Conceptualization. **Jesús Pérez-Gil:** Writing – review & editing, Supervision, Resources, Project administration, Formal analysis, Conceptualization.

Acknowledgements

The authors acknowledge the collaboration of Dr. Alberto Galindo and Dr. Emma Batllori-Badia, from the Obstetrics and Gynaecology Department of Hospital “12 de Octubre” from Madrid, in the obtention of the AFS samples, always under a protocol approved by the Ethical Committee of the Hospital (22/108). This work was funded by the Spanish Ministry of Science and Innovation through grants PID2021-124932OB-I00 and PID2024-156556OB-I00.

Data availability

Data will be made available on request.

References

Adams, F.H., Towers, B., Osher, A.B., Ikegami, M., Fujiwara, T., Nozaki, M., 1978. Effects of tracheal instillation of natural surfactant in premature lambs. I. Clinical and autopsy findings. Pediatr. Res. 12 (8), 841–848. https://doi.org/10.1203/00006450-197808000-00008.

Autilio, C., Echaide, M., Benachi, A., Marfaing-Koka, A., Capoluongo, E.D., Pérez-Gil, J., De Luca, D., 2017. A Noninvasive surfactant adsorption test predicting the need for surfactant therapy in preterm infants treated with continuous positive airway pressure. J. Pediatr. 182, 66–73. https://doi.org/10.1016/j.jpeds.2016.11.057 e61.

Baer, B., Souza, L.M.P., Pimentel, A.S., Veldhuizen, R.A.W., 2019. New insights into exogenous surfactant as a carrier of pulmonary therapeutics. Biochem. Pharmacol. 164, 64–73. https://doi.org/10.1016/j.bcp.2019.03.036.

Bjermer, L., Lundgren, R., Hällgren, R., 1989. Hyaluronan and type III procollagen peptide concentrations in bronchoalveolar lavage fluid in idiopathic pulmonary fibrosis. Thorax 44 (2), 126–131. https://doi.org/10.1136/thx.44.2.126.

Braun, A., Stenger, P.C., Warriner, H.E., Zasadzinski, J.A., Lu, K.W., Taeusch, H.W., 2007. A freeze-fracture transmission electron microscopy and small angle x-ray diffraction study of the effects of albumin, serum, and polymers on clinical lung surfactant microstructure. Biophys. J. 93 (1), 123–139. https://doi.org/10.1529/biophysj.106.095513.

Castillo-Sánchez, J.C., Collada, A., Batllori-Badia, E., Galindo, A., Cruz, A., Pérez-Gil, J., 2025. The pristine unused pulmonary surfactant isolated from human amniotic fluid forms highly condensed interfacial films. Physiol. Rep. 13 (12), e70403. https://doi.org/10.14814/phy2.70403.

Castillo-Sánchez, J.C., Roldán, N., García-Álvarez, B., Batllori, E., Galindo, A., Cruz, A., Pérez-Gil, J., 2022. The highly packed and dehydrated structure of preformed unexposed human pulmonary surfactant isolated from amniotic fluid. Am. J. Physiol. Lung Cell Mol. Physiol. 322 (2), L191–l203. https://doi.org/10.1152/ajplung.00230.2021.

Cerrada, A., Haller, T., Cruz, A., Pérez-Gil, J., 2015. Pneumocytes Assemble Lung Surfactant as Highly Packed/Dehydrated States with Optimal Surface Activity. Biophys. J. 109 (11), 2295–2306. https://doi.org/10.1016/j.bpj.2015.10.022.

Chung, J., Yu, S.H., Whitsett, J.A., Harding, P.G., Possmayer, F., 1989. Effect of surfactant-associated protein-A (SP-A) on the activity of lipid extract surfactant. Biochim. Biophys. Acta 1002 (3), 348–358. https://doi.org/10.1016/0005-2760(89)90349-4.

Echaide, M., Autilio, C., Arroyo, R., Perez-Gil, J., 2017. Restoring pulmonary surfactant membranes and films at the respiratory surface. Biochim. Biophys. Acta Biomembr. 1859 (9 Pt B), 1725–1739. https://doi.org/10.1016/j.bbamem.2017.03.015.

Enhörning, G., Robertson, B., 1972. Lung expansion in the premature rabbit fetus after tracheal deposition of surfactant. Pediatrics 50 (1), 58–66.

Fujiwara, T., Maeta, H., Chida, S., Morita, T., Watabe, Y., Abe, T., 1980. Artificial surfactant therapy in hyaline-membrane disease. Lancet 1 (8159), 55–59. https://doi.org/10.1016/s0140-6736(80)90489-4.

García-Mouton, C., Echaide, M., Serrano, L.A., Orellana, G., Salomone, F., Ricci, F., Pioselli, B., Amidani, D., Cruz, A., Pérez-Gil, J., 2023. Beyond the Interface: improved Pulmonary Surfactant-Assisted Drug Delivery through Surface-Associated Structures. Pharmaceutics 15 (1). https://doi.org/10.3390/pharmaceutics15010256.

Hällgren, R., Samuelsson, T., Laurent, T.C., Modig, J., 1989. Accumulation of hyaluronan (hyaluronic acid) in the lung in adult respiratory distress syndrome. Am. Rev. Respir. Dis. 139 (3), 682–687. https://doi.org/10.1164/ajrccm/139.3.682.

Henkel, A.W., Lübke, J., Betz, W.J., 1996. FM1-43 dye ultrastructural localization in and release from frog motor nerve terminals. Proc. Natl. Acad. Sci. U S. A 93 (5), 1918–1923. https://doi.org/10.1073/pnas.93.5.1918.

Hidalgo, A., Garcia-Mouton, C., Autilio, C., Carravilla, P., Orellana, G., Islam, M.N., Bhattacharya, J., Bhattacharya, S., Cruz, A., Pérez-Gil, J., 2021. Pulmonary surfactant and drug delivery: vehiculization, release and targeting of surfactant/tacrolimus formulations. J. Control. Release: Off. J. Control. Release Soc. 329, 205–222. https://doi.org/10.1016/j.jconrel.2020.11.042.

Hidalgo, A., Salomone, F., Fresno, N., Orellana, G., Cruz, A., Perez-Gil, J., 2017. Efficient Interfacially Driven Vehiculization of Corticosteroids by Pulmonary Surfactant. Langmuir. 33 (32), 7929–7939. https://doi.org/10.1021/acs.langmuir.7b01177.

Hobi, N., Siber, G., Bouzas, V., Ravasio, A., Pérez-Gil, J., Haller, T., 2014. Physiological variables affecting surface film formation by native lamellar body-like pulmonary surfactant particles. Biochim. Biophys. Acta 1838 (7), 1842–1850. https://doi.org/10.1016/j.bbamem.2014.02.015.

Kobayashi, T., Ohta, K., Tashiro, K., Nishizuka, K., Chen, W.M., Ohmura, S., Yamamoto, K., 1999. Dextran restores albumin-inhibited surface activity of pulmonary surfactant extract. J. Appl. Physiol. 86 (6), 1778–1784. https://doi.org/10.1152/jappl.1999.86.6.1778. *1985*.

Lopez-Rodriguez, E., Cruz, A., Richter, R.P., Taeusch, H.W., Pérez-Gil, J., 2013. Transient exposure of pulmonary surfactant to hyaluronan promotes structural and compositional transformations into a highly active state. J. Biol. Chem. 288 (41), 29872–29881. https://doi.org/10.1074/jbc.M113.493957.

López-Rodríguez, E., Ospina, O.L., Echaide, M., Taeusch, H.W., Pérez-Gil, J., 2012. Exposure to polymers reverses inhibition of pulmonary surfactant by serum, meconium, or cholesterol in the captive bubble surfactometer. Biophys. J. 103 (7), 1451–1459. https://doi.org/10.1016/j.bpj.2012.08.024.

López-Rodríguez, J.C., Barderas, R., Echaide, M., Pérez-Gil, J., Villalba, M., Batanero, E., Cruz, A., 2016. Surface activity as a crucial factor of the biological Actions of Ole e 1, the main aeroallergen of olive tree (Olea europaea) Pollen. Langmuir 32 (42), 11055–11062. https://doi.org/10.1021/acs.langmuir.6b02831.

Lu, K.W., Goerke, J., Clements, J.A., Taeusch, H.W., 2005a. Hyaluronan decreases surfactant inactivation in vitro. Pediatr. Res. 57 (2), 237–241. https://doi.org/10.1203/01.Pdr.0000150726.75308.22.

Lu, K.W., Goerke, J., Clements, J.A., Taeusch, H.W., 2005b. Hyaluronan reduces surfactant inhibition and improves rat lung function after meconium injury. Pediatr. Res. 58 (2), 206–210. https://doi.org/10.1203/01.Pdr.0000169981.06266.3e.

Lu, K.W., Pérez-Gil, J., Taeusch, H., 2009. Kinematic viscosity of therapeutic pulmonary surfactants with added polymers. Biochim. Biophys. Acta 1788 (3), 632–637. https://doi.org/10.1016/j.bbamem.2009.01.005.

Lu, K.W., Taeusch, H.W., 2010. Combined effects of polymers and KL(4) peptide on surface activity of pulmonary surfactant lipids. Biochim. Biophys. Acta 1798 (6), 1129–1134. https://doi.org/10.1016/j.bbamem.2010.02.026.

Morley, C., Robertson, B., Lachmann, B., Nilsson, R., Bangham, A., Grossmann, G., Miller, N., 1980. Artificial surfactant and natural surfactant. Comparative study of the effects on premature rabbit lungs. Arch. Dis. Child 55 (10), 758–765. https://doi.org/10.1136/adc.55.10.758.

Ravasio, A., Cruz, A., Pérez-Gil, J., Haller, T., 2008. High-throughput evaluation of pulmonary surfactant adsorption and surface film formation. J. Lipid Res. 49 (11), 2479–2488. https://doi.org/10.1194/jlr.D800029-JLR200.

Ravasio, A., Olmeda, B., Bertocchi, C., Haller, T., Pérez-Gil, J., 2010. Lamellar bodies form solid three-dimensional films at the respiratory air-liquid interface. J. Biol. Chem. 285 (36), 28174–28182. https://doi.org/10.1074/jbc.M110.106518.

Rouser, G., Siakotos, A.N., Fleischer, S., 1966. Quantitative analysis of phospholipids by thin-layer chromatography and phosphorus analysis of spots. Lipids 1 (1), 85–86. https://doi.org/10.1007/bf02668129.

Rüdiger, M., Tölle, A., Meier, W., Rüstow, B., 2005. Naturally derived commercial surfactants differ in composition of surfactant lipids and in surface viscosity. Am. J. Physiol. Lung Cell Mol. Physiol. 288 (2), L379–L383. https://doi.org/10.1152/ajplung.00176.2004.

Sahu, S.C., Tanswell, A.K., Lynn, W.S., 1980. Isolation and characterization of glycosaminoglycans secreted by human foetal lung type II pneumocytes in culture. J. Cell Sci. 42, 183–188. https://doi.org/10.1242/jcs.42.1.183.

Schneider, H.A., Hallman, M., Benirschke, K., Gluck, L., 1982. Human surfactant: a therapeutic trial in premature rabbits. J. Pediatr. 100 (4), 619–622. https://doi.org/10.1016/s0022-3476(82)80769-5.

Schoel, W.M., Schürch, S., Goerke, J., 1994. The captive bubble method for the evaluation of pulmonary surfactant: surface tension, area, and volume calculations. Biochim. Biophys. Acta 1200 (3), 281–290. https://doi.org/10.1016/0304-4165(94)90169-4.

Schürch, D., Ospina, O.L., Cruz, A., Pérez-Gil, J., 2010. Combined and independent action of proteins SP-B and SP-C in the surface behavior and mechanical stability of pulmonary surfactant films. Biophys. J. 99 (10), 3290–3299. https://doi.org/10.1016/j.bpj.2010.09.039.

Scott, J.E., Cummings, C., Brass, A., Chen, Y., 1991. Secondary and tertiary structures of hyaluronan in aqueous solution, investigated by rotary shadowing-electron microscopy and computer simulation. Hyaluronan is a very efficient network-forming polymer. Biochem. J. 274 (Pt 3), 699–705. https://doi.org/10.1042/bj2740699. Pt 3.

Seurynck-Servoss, S.L., Brown, N.J., Dohm, M.T., Wu, C.W., Barron, A.E., 2007. Lipid composition greatly affects the in vitro surface activity of lung surfactant protein mimics. Colloids Surf. B Biointerfaces 57 (1), 37–55. https://doi.org/10.1016/j.colsurfb.2007.01.001.

Stenger, P.C., Zasadzinski, J.A., 2007. Enhanced surfactant adsorption via polymer depletion forces: a simple model for reversing surfactant inhibition in acute respiratory distress syndrome. Biophys. J. 92 (1), 3–9. https://doi.org/10.1529/biophysj.106.091157.

Taeusch, H.W., Bernardino de la Serna, J., Perez-Gil, J., Alonso, C., Zasadzinski, J.A., 2005. Inactivation of pulmonary surfactant due to serum-inhibited adsorption and reversal by hydrophilic polymers: experimental. Biophys. J. 89 (3), 1769–1779. https://doi.org/10.1529/biophysj.105.062620.

Taeusch, H.W., Dybbro, E., Lu, K.W., 2008. Pulmonary surfactant adsorption is increased by hyaluronan or polyethylene glycol. Colloids Surf. B Biointerfaces 62 (2), 243–249. https://doi.org/10.1016/j.colsurfb.2007.10.009.

Turino, G.M., Cantor, J.O., 2003. Hyaluronan in respiratory injury and repair. Am. J. Respir. Crit. Care Med. 167 (9), 1169–1175. https://doi.org/10.1164/rccm.200205-449PP.

Weaver, T.E., Na, C.L., Stahlman, M., 2002. Biogenesis of lamellar bodies, lysosome-related organelles involved in storage and secretion of pulmonary surfactant. Semin. Cell Dev. Biol. 13 (4), 263–270. https://doi.org/10.1016/s1084952102000551.

Whitsett, J.A., Ohning, B.L., Ross, G., Meuth, J., Weaver, T., Holm, B.A., Shapiro, D.L., Notter, R.H., 1986. Hydrophobic surfactant-associated protein in whole lung surfactant and its importance for biophysical activity in lung surfactant extracts used for replacement therapy. Pediatr. Res. 20 (5), 460–467. https://doi.org/10.1203/00006450-198605000-00016.

William Taeusch, H., Lu, K.W., Goerke, J., Clements, J.A., 1999. Nonionic polymers reverse inactivation of surfactant by meconium and other substances. Am. J. Respir. Crit. Care Med. 159 (5 Pt 1), 1391–1395. https://doi.org/10.1164/ajrccm.159.5.9808047.

Willson, D.F., Notter, R.H., 2011. The future of exogenous surfactant therapy. Respir. Care 56 (9), 1369–1386. https://doi.org/10.4187/respcare.01306 discussion 1386-1368.

Yadav, R., Sivoria, N., Maiti, S., 2024. Salt Gradient-Induced Phoresis of Vesicles and Enhanced Membrane Fusion in a Crowded Milieu. J. Phys. Chem. B 128 (39), 9573–9585. https://doi.org/10.1021/acs.jpcb.4c03985.

Zuo, Y.Y., Alolabi, H., Shafiei, A., Kang, N., Policova, Z., Cox, P.N., Acosta, E., Hair, M.L., Neumann, A.W., 2006. Chitosan enhances the in vitro surface activity of dilute lung surfactant preparations and resists albumin-induced inactivation. Pediatr. Res. 60 (2), 125–130. https://doi.org/10.1203/01.pdr.0000227558.14024.57.